Topological Locating of Power Quality Event Source

Dong-Jun Won† and Seung-Il Moon*

Abstract - This paper proposes a topological locating algorithm to determine the location of the power quality event source. This algorithm makes use of the information on the topology of the monitored network and on the direction of PQ events. As a result, the bus incidence matrix is modified using monitor location and the direction matrix is constructed. With this information, the algorithm determines the suspected locations of the PQ events. To reduce suspicious areas, it utilizes event cause and related equipment. In case of line fault event, it calculates the distance from the monitor to the location of event source. The overall algorithm is applied to the IEEE test feeder and accurately identifies the event source location.

Keywords: distribution system, event, fault, harmonics, monitoring, power quality, sag

1. Introduction

In the past, power quality (PQ) had been recognized as the ability of utilities to provide electric power without interruption. Due to the increase in critical loads and electronic devices, the issue of power quality has become an important concern to customers as well as utilities and facilities. It is these growing concerns about PQ problems that make the PQ monitoring system so essential nowadays [1].

Most power quality monitoring systems are adopting the power quality diagnosis function as their premium service. The PQ diagnosis function can provide the cause and effect of individual PQ problems, allowing customers to solve their PQ problems more easily. Among various diagnosis functions, event source locating is fairly significant because it can determine who is responsible for the event and how the event can be solved.

A few papers have dealt with the method to find the location of the PQ event [2-5]. Because these methods usually utilize the information acquired at one monitoring point, they have some limitations in identifying the exact location of the PQ event source. These methods can only determine the relative position of the PQ event source at the monitoring point, that is, the upper-side event or down-side event. These methods should be extended to analyze the information at multiple monitoring points together [6, 7] in order to determine the accurate location of the PQ event.

Therefore, this paper presents a systematic algorithm to locate the PQ event source. Using the power system tree structure, the relation between system topology and monitor location is expressed in a matrix form. Relative location of the PQ event is also determined and expressed in a matrix form. The suspicious area is identified using these two matrices and reduced further using event cause and fault distance. The proposed algorithm is clearly illustrated and verified using an example system. Finally, this algorithm is applied to an IEEE test feeder in order to validate its effectiveness.

† Corresponding Author: School of Electrical Engineering, INHA University, Incheon 402-751, Korea (djwon@inha.ac.kr).
* School of Electrical Engineering and Computer Science, Seoul National University, Seoul 151-742, Korea (moonsi@plaza.snu.ac.kr).
Received April 14, 2005 ; Accepted September 14, 2005

2. Locating of Event Source using System Topology

2.1 Tree Representation

In power system analysis, the graph theory and incidence matrices have been frequently used for computer simulation [8]. Especially, tree structure [9] is an effective methodology for the representation of a radial distribution system. Therefore, the tree structure is adopted in this

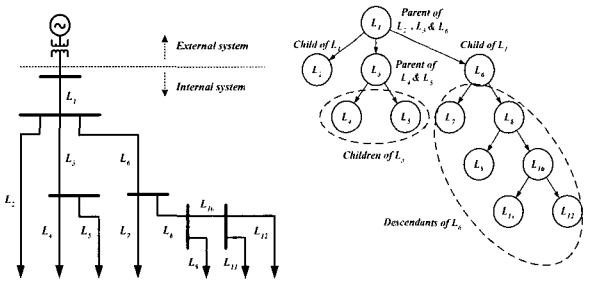

(a) (b)

Fig. 1 Rooted tree representation of example system (a) One-line diagram of example system for rooted tree (b) Rooted tree representation and parent-child relationship

paper to develop an event source locating algorithm in a radial distribution system. The components in the power system become the nodes of a rooted tree and are numbered in Fig. 1.

In Fig. 1(a), L_1 becomes the root of the tree. For L_1 is connected with L_2, L_3 and L_6 in Fig. 1(a), the node L_1 is connected with the node L_2, L_3 and L_6 in Fig. 1(b). Other nodes are connected with one another in this way. In the rooted tree, there is a parent-child relationship between nodes. For example, L_1 is the parent of L_2, L_3 and L_6. L_3 is the parent of L_4 and L_5. L_4 and L_5 are the children of L_3. In this way, $L_7 \sim L_{12}$ become the descendants of L_6. These relationships will be used later to construct a modified incidence matrix.

2.2 Up/Down Area Definition

If a monitor is installed in a power system, the monitor can identify the relative location of the event source [4, 5]. In other words, the monitor can determine whether the event has come from the UP area or the DOWN area. The relative location of the event source is classified into UP area and DOWN area. From an electrical viewpoint, the power always flows from source to load through the power quality monitor in a radial distribution system. Therefore, the DOWN area can be defined as the area to which the power flows from the monitoring point. The UP area is the other area that is not included in DOWN area, that is, the area from which the power flows to the monitoring point and their regional area.

2.3 Coverage Matrix

Once the monitors are located within a power system, the UP/DOWN area according to the monitor location is uniquely determined. This means that the bus incidence matrix can be modified considering the monitor locations. If the monitor location replaces the bus locations in the bus incidence matrix, the modified incidence matrix can be obtained, which is called *'coverage matrix'*.

Coverage matrix informs us of the relation between the monitor and the component. It indicates whether the component is in the UP or DOWN area of a monitor. In other words, it reveals the coverage of the monitors. The coverage matrix is $L \times M$ matrix. L represents the number of lines and M represents the number of monitors. The elements of the coverage matrix are determined as follows.

In Fig. 2, a total of 5 monitors are located in the example system. The resulting coverage matrix is (1). In (1), for M_1 is installed at L_1, a_{11} is +1. Other elements which are the descendants of L_1 are all set to +1, that is, $a_{21} \sim a_{121}$ are all +1. For M_2 is installed at L_2 and L_2 has no descendants, only a_{22} is +1. For M_3 is installed at L_3, a_{33} is +1. Because L_4 and L_5 are the descendants of L_3, a_{43} and a_{53} are also +1. Similarly, other elements of the matrix are determined.

$$a_{ij} = \begin{cases} +1 & \text{if } i_{th} \text{ component is in DOWN area of } j_{th} \text{ monitor} \\ -1 & \text{if } i_{th} \text{ component is in UP area of } j_{th} \text{ monitor} \end{cases}$$

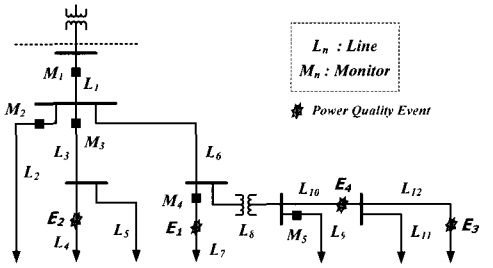

Fig. 2 Monitor and event locations in example system

$$\text{Coverage matrix} = \begin{array}{c} c \backslash m \\ L_1 \\ L_2 \\ L_3 \\ L_4 \\ L_5 \\ L_6 \\ L_7 \\ L_8 \\ L_9 \\ L_{10} \\ L_{11} \\ L_{12} \end{array} \begin{array}{c} M_1 \quad M_2 \quad M_3 \quad M_4 \quad M_5 \\ \left[\begin{array}{ccccc} +1 & -1 & -1 & -1 & -1 \\ +1 & +1 & -1 & -1 & -1 \\ +1 & -1 & +1 & -1 & -1 \\ +1 & -1 & +1 & -1 & -1 \\ +1 & -1 & +1 & -1 & -1 \\ +1 & -1 & -1 & -1 & -1 \\ +1 & -1 & -1 & +1 & -1 \\ +1 & -1 & -1 & -1 & -1 \\ +1 & -1 & -1 & -1 & +1 \\ +1 & -1 & -1 & -1 & -1 \\ +1 & -1 & -1 & -1 & -1 \\ +1 & -1 & -1 & -1 & -1 \end{array}\right] \end{array} \quad (1)$$

2.4 Direction Matrix

If the event direction is identified in power quality monitors, the results should be stored in matrix form for use in computing the algorithm. The *'direction matrix'* is introduced for this purpose in this section. The direction matrix includes information about the directions of an event at the monitoring points. This information is generated at the monitors when a power quality event happens as mentioned before. The dimension of the direction matrix is $M \times 1$. The elements of the direction matrix are as follows.

$$a_i = \begin{cases} +1 & \text{if monitor } i \text{ detects DOWN event} \\ -1 & \text{if monitor } i \text{ detects UP event} \end{cases}$$

For example, 4 events are assumed to occur in the example system shown in Fig. 2. If each event takes place respectively at L_7, L_2, L_{12} and L_{10}, each monitor will determine the directions of these events. The results are shown in Table 1.

Table 1 Results of event direction identification

Event / Result	Event at L_7	Event at L_2	Event at L_{12}	Event at L_{10}
Direction ($M_1/M_2/M_3/M_4/M_5$)	DN/UP/UP/DN/UP	DN/UP/DN/UP/UP	DN/UP/UP/UP/UP	DN/UP/UP/UP/UP

Then, the direction matrix that corresponds to Table 1 will be M_{D1}, M_{D2}, M_{D3} and M_{D4} in (2). The direction matrix will have further application in calculating the candidate matrix. This will be discussed in the following chapter.

$$M_{D1}=\begin{bmatrix}+1\\-1\\-1\\+1\\-1\end{bmatrix}\quad M_{D2}=\begin{bmatrix}+1\\-1\\+1\\-1\\-1\end{bmatrix}\quad M_{D3}=\begin{bmatrix}+1\\-1\\-1\\-1\\-1\end{bmatrix}\quad M_{D4}=\begin{bmatrix}+1\\-1\\-1\\-1\\-1\end{bmatrix} \tag{2}$$

2.5 Candidate Matrix

Multiplication of coverage matrix and direction matrix makes the candidate matrix.

$$M_C=\frac{1}{M}\cdot M_{co}\cdot M_D \tag{3}$$

where,

M_C: *candidate matrix* $(L\times 1)$
M_{co}: *coverage matrix* $(L\times M)$
M_D: *direction matrix* $(M\times 1)$
M: *total number of monitor*
L: *total number of component*

'*Candidate matrix*' is a normalized $L\times 1$ matrix. It represents the suspicious area where an event source may exist. If a row element of this matrix is equal to unity, then the component corresponding to this row can be a possible candidate of the event source location. If such a row is unique as shown in M_{C1} in (4), the corresponding branch is the accurate location of the event source. If there are multiple rows equal to unity, the location of the event source cannot be identified uniquely. In this case, the exact location exists among such branches. Further investigation using component locating or fault distance calculation is needed.

$$M_{C1}=\begin{bmatrix}0.6\\0.2\\0.2\\0.2\\0.2\\0.6\\\underline{1.0}\\0.6\\0.2\\0.6\\0.6\\0.6\end{bmatrix}\quad M_{C2}=\begin{bmatrix}0.6\\0.2\\\underline{1.0}\\\underline{1.0}\\\underline{1.0}\\0.6\\0.2\\0.6\\0.2\\0.6\\0.6\\0.6\end{bmatrix}\quad M_{C3}=\begin{bmatrix}\underline{1.0}\\0.6\\0.6\\0.6\\0.6\\\underline{1.0}\\0.6\\\underline{1.0}\\0.6\\\underline{1.0}\\\underline{1.0}\\\underline{1.0}\end{bmatrix}\quad M_{C4}=\begin{bmatrix}\underline{1.0}\\0.6\\0.6\\0.6\\0.6\\\underline{1.0}\\0.6\\\underline{1.0}\\0.6\\\underline{1.0}\\\underline{1.0}\\\underline{1.0}\end{bmatrix} \tag{4}$$

3. Component Locating

3.1 Relating Event Causes with Equipments

If multiple components are selected in the candidate matrix, the suspicious areas should be reduced to obtain a more accurate location. Because the event cause has a close relation with the equipment that causes the event, the suspicious area can be reduced by inspecting the event cause. Table 2 shows the event causes and related equipments which cause them.

Table 2 Event Causes And Related Equipments

	Causes	***Equipment***
Voltage variation event	*Line fault*	*Distribution line (Main feeder, lateral line)*
	Induction motor starting	*Induction motor*
	Transformer saturation	*Transformer*
Harmonic event	*6 pulse converter switching*	*6 pulse converter*
	12 pulse converter switching	*12 pulse converter*
	Other nonlinear loads	*Transformer, etc*

3.2 Reduction of Suspicious Areas

The event source location can be identified by matching the event cause and equipment in suspicious areas. For example, if the event cause is harmonics and there is only one converter in the suspicious area, then the converter is thought of as the event source. Especially, in the case of a voltage variation event due to induction motor starting, the rating of the motor is also utilized to distinguish the location of an event source from multiple induction motors. The induction motor that has the most similar rating with the calculated rating will be thought of as the event source. If the suspicious area consists of only distribution lines, it is impossible to reduce the suspicious area further. At this time, the necessity for fault distance calculation arises. The following section describes the details of fault distance calculation.

4. Fault Distance Calculation

If the cause of event is voltage variation and there are

multiple lines in the suspicious area, then the fault distance calculation is needed. Fig. 3 shows the equivalent circuit to calculate the fault distance in case of a single line to ground fault.

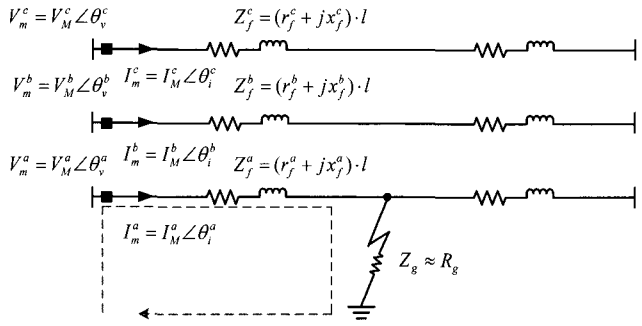

Fig. 3 Equivalent circuit to calculate fault distance

In this figure, V_m^a, V_m^b, V_m^c and I_m^a, I_m^b, I_m^c are the voltages and currents measured at the monitor. Z_f^a, Z_f^b, Z_f^c are line impedances from monitor to fault location and l is corresponding distance. $r_f^a + jx_f^a$, $r_f^b + jx_f^b$, $r_f^c + jx_f^c$ are the line impedances per unit length. Z_g is fault impedance to ground at the fault location. Because fault impedance is generally thought to have only a resistive component, it can also be approximated to R_g. Following the loop in Fig. 3, (5) is obtained by KVL (Kirchhoff's Voltage Law).

$$Z_f^a = \frac{V_m^a}{I_m^a} - Z_g \tag{5}$$

Because (5) consists of a complex variable, it can be divided into real part equation and imaginary part equation. (6) and (7) are the equations obtained by separating the real and imaginary part of (5).

$$r_f^a \cdot l = \frac{V_M^a}{I_M^a}\cos(\theta_v^a - \theta_i^a) - R_g \tag{6}$$

$$x_f^a \cdot l = \frac{V_M^a}{I_M^a}\sin(\theta_v^a - \theta_i^a) \tag{7}$$

In (7), all the variables are already known except the fault distance l. Therefore, the fault distance can be obtained from (7). After the calculation of fault distance, the fault impedance R_g can be computed from (6) using the fault distance l.

$$l = \frac{V_M^a \cdot \sin(\theta_v^a - \theta_i^a)}{I_M^a \cdot x_f^a} \tag{8}$$

$$R_g = \frac{V_M^a}{I_M^a}\cos(\theta_v^a - \theta_i^a) - r_f^a \cdot \frac{V_M^a \cdot \sin(\theta_v^a - \theta_i^a)}{I_M^a \cdot x_f^a} \tag{9}$$

Similar to the case of a single line to ground fault, a three line to ground fault requires the same equation. (8) and (9) are extended to three phase in case of a three line to ground fault. The fault distance and fault impedance are the averages of those of each phase.

$$l = \frac{l^a + l^b + l^c}{3} \tag{10}$$

$$R_g = \frac{R_g^a + R_g^b + R_g^c}{3} \tag{11}$$

5. Case Study

5.1 Test System

In this chapter, the overall event source identification algorithm is applied to an IEEE 13 node test feeder. The IEEE 13 node test feeder is one of the radial distribution feeders that are developed for computer simulation by the IEEE Distribution System Analysis Subcommittee [10]. Fig. 4 shows the test system developed using PSCAD/EMTDC™. A total of 5 monitors are installed in the test case system and each event location is indicated in Fig. 4.

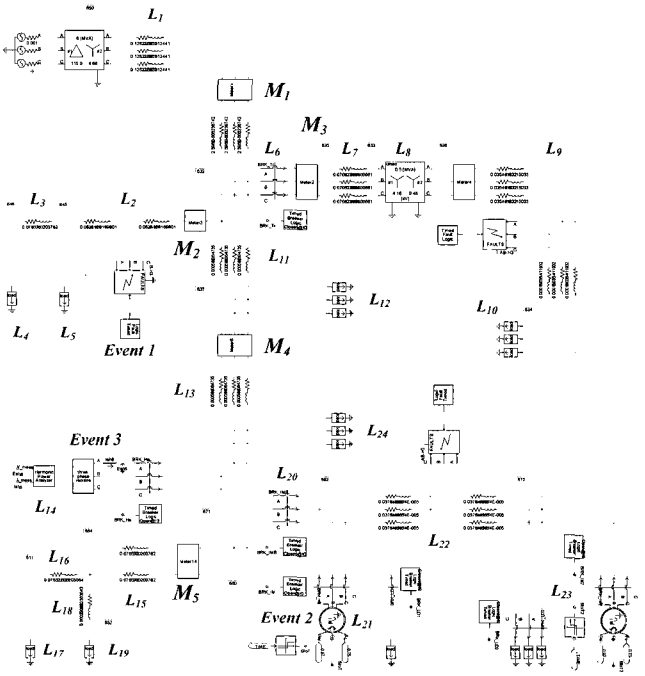

Fig. 4 IEEE 13 node test feeder modified for case study

5.2 Event Description

For the case study, 3 different events are assumed to happen in the test case system. Each event is chosen to validate the event source identification algorithm most effectively. Table 3 describes each event.

Table 3 Case descriptions used in case study

Description / Case Num.	Cause	Location
Case 1	*One line to ground fault*	L_2 *(250 ft)*
Case 2	*Induction motor starting*	L_{21}
Case 3	*Harmonic distortion due to 6 pulse converter*	L_{14}

In case 1, one line to ground fault occurs at L_2 to verify the overall algorithm of the event source identification including the fault distance calculation. In case 2, the induction motor starts at L_{21} to verify the component locating algorithm in an induction motor event. In case 3, a 6 pulse converter operates and injects harmonics into the system.

5.3 Results and Analysis

Case 1: One line to ground fault at L_2 (250 ft)

As shown in Fig. 5, voltage sag happens and large fault current flows. The event cause is determined as the line fault and the direction is identified as the DOWN side of M_1 and M_2. The suspicious area is determined as (L_2, L_3, L_4, L_5). Because the components that correspond to the line fault are L_2 and L_3, the fault distance calculation is performed for these two lines. As shown in Table 4, the fault location has been accurately decided and the error is below 1% of the actual value.

Because of the increase of steady state power in all phases, the event cause becomes induction motor starting and the direction is DOWN at M_4. However, because the power does not increase in M_3, the direction becomes UP at M_3. The suspicious area is determined as (L_{13}, L_{14}, L_{20}, L_{21}, L_{22}, L_{23}, L_{24}). Because the components that correspond to the event cause are L_{21} and L_{23} by component locating, the motor rating is utilized in such a case. When the estimated load increase at M_4 is 0.6875 MVA, the event location is determined as L_{21}.

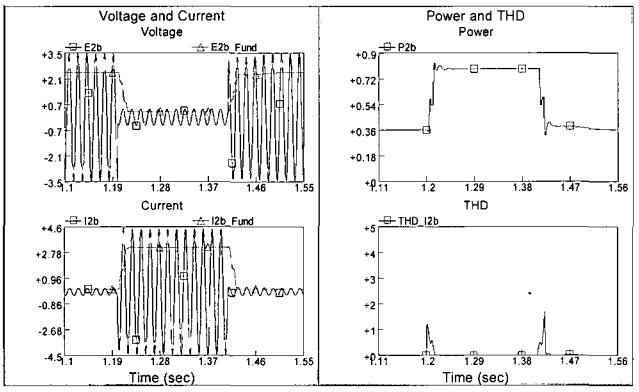

Fig. 5 Monitored parameters at M_2 (DOWN_LF)

Table 4 Estimated fault distance and decision

Value / Result	Actual	Estimated	Error (%)	Decision
Distance	*250 ft*	*250.335 ft*	*0.134*	L_2
Fault impedance	*0.0173 ohm*	*0.0174 ohm*	*0.578*	

Case 2: Induction motor starting at L_{21}

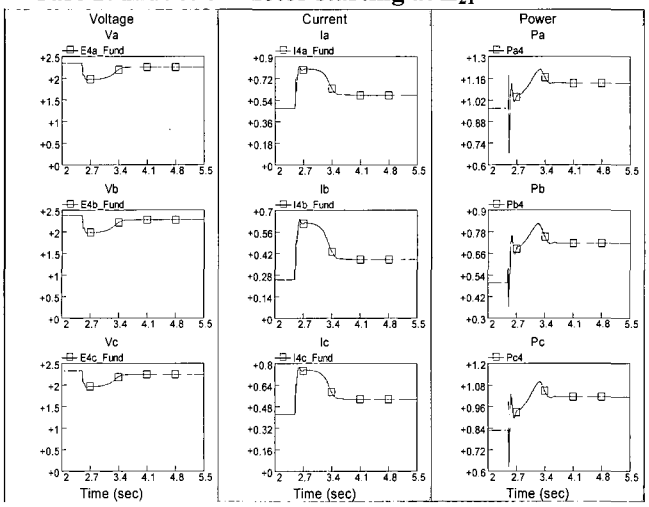

Fig. 6 Monitored parameters at M_4 (DOWN_IM)

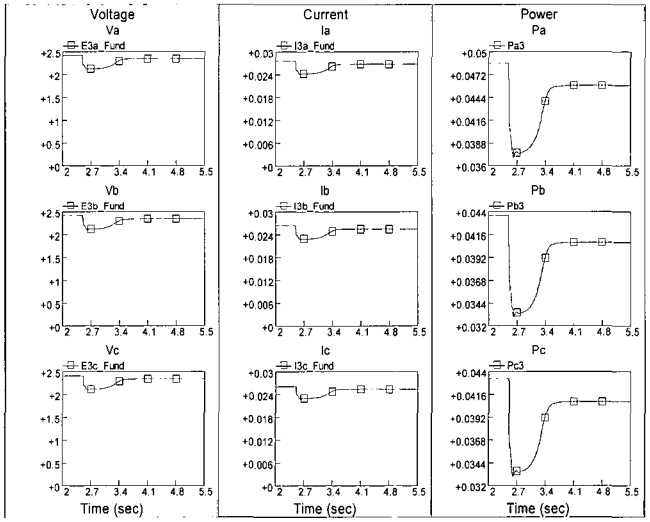

Fig. 7 Monitored parameters at M_3 (UP)

Table 5 Estimated load increase and decision

component / Rating	Calculated	L_{21}	L_{23}	Decision
Rating	*0.6875 MVA*	*0.8 MVA*	*0.3 MVA*	L_{21}

Case 3: Harmonic distortion due to 6 pulse converter switching at L_{14}

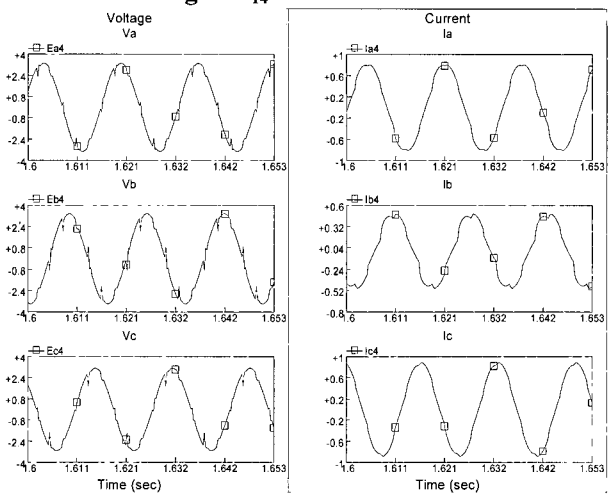

Fig. 8 Monitored parameters at M_4 (DOWN_HD)

The largest harmonic contents are 5th, 7th, 11th and 17th at all monitors. Therefore, the event cause is determined as 6 pulse converter switching. The suspicious area is determined as (L_{13}, L_{14}, L_{20}, L_{21}, L_{22}, L_{23}, L_{24}). Because the component which corresponds to the event cause is only L_{14}, the event location becomes L_{14}.

6. Conclusion

This paper has presented a topological locating algorithm to determine the location of the PQ event source. The coverage matrix and the direction matrix have been developed and the candidate matrix has been calculated using these two matrices. The suspicious area for the event source has been determined from the candidate matrix. Component locating, which utilizes event cause and related equipment, has reduced the suspicious area. The fault distance also helps to identify the event location more accurately. The overall event source locating algorithm has been applied to an IEEE 13 node test feeder and it has produced fairly accurate results as supposed.

Acknowledgements

This work was supported by 2006 INHA UNIVERSITY Research Grant (INHA-34381).

References

[1] Mark McGranaghan, "Trends in Power Quality Monitoring," IEEE Power Engineering Review, vol. 21, Issue 10, pp. 3-9, 21, Oct. 2001.

[2] G. T. Heydt, "Identification of Harmonic Sources by a State Estimation Technique," IEEE Trans. Power Delivery, vol. 4, no. 1, pp. 569-576, Jan. 1989

[3] Astrat Teshome, "Harmonic Source and Type Identification in a Radial Distribution System," Conference Record of the 1991 IEEE Industrial Applications Society Annual Meeting, vol. 2, pp. 1605-1609, 1991.

[4] Anthony C. Parsons, W. Mack Grady, Edward J. Powers, John C. Soward, "Rules for Locating the Sources of Capacitor Switching Disturbances," IEEE Power Engineering Society Summer Meeting, vol. 2, pp. 794-799, 1999.

[5] Anthony C. Parsons, W. Mack Grady, Edward J. Powers, John C. Soward, "A Direction Finder for Power Quality Disturbances Based Upon Disturbance Power and Energy," IEEE Trans. Power Delivery, vol. 15, no. 3, pp. 1081-1086, July 2000.

[6] L. Cristaldi, A. Ferrero, S. Salicone, "A Distributed System for Electric Power Quality Measurement," *IEEE Transactions on Instrumentation and Measurement*, vol. 51, no. 4, pp. 776 -781, Aug. 2002.

[7] Ben Byman, Tom Yarborough, Rudolf Schnorr von Carolsfeld, John Van Gorp, "Using Distributed Power Quality Monitoring for Better Electrical System Management," *IEEE Transactions on Industry Applications*, vol. 36, no. 5, pp. 1481-1485, Sep.-Oct. 2000.

[8] Glenn W. stagg, Ahmed H. El-Abiad, Computer methods in power systems analysis, New York: Mcgraw-Hill, Inc., 1968.

[9] Mark Allen Weiss, Data Structures & Problem Solving using JAVA™, 2nd ed., Addison Wesley, Inc., 2002, pp. 570.

[10] Distribution System Analysis Subcommittee Report, Radial Distribution Test Feeders, http://ewh.ieee.org/soc/pes/dsacom/testfeeders.html

Dong-Jun Won

He received his B.S., M.S. and Ph.D. degrees in Electrical Engineering from Seoul National University, Seoul, Korea in 1998, 2000 and 2004 respectively. Previously, he was a Postdoctoral Fellow with the APT Center, University of Washington, Seattle, USA. He is currently a full-time lecturer in the School of Electrical Engineering at INHA University. His special fields of interest include power quality, dispersed generation, renewable energy and hydrogen economy.

Seung-Il Moon

He received his B.S. degree in Electrical Engineering from Seoul National University, Seoul, Korea in 1985. He received his M.S. and Ph. D. degrees in Electrical Engineering from Ohio State University in 1989 and 1993, respectively. Currently, he is an Associate Professor at the School of Electrical Engineering and Computer Science at Seoul National University. His special fields of interest include power quality, FACTS, renewable energy and dispersed generation.